



Growth, studies of milled and irradiated crystalline samples of DBNT for macro-photonic and electro-mechano functionalities

Meena M^a, SenthilKannan K^{b,*}, Mohammed S. Alqahtani^{c,d}, Mohamed Abbas^{e,f}

^a Department of Chemistry, R.M.K Engineering College, Kavaraipettai, Thiruvallur, 601 206, Tamilnadu, India

^b Department of Physics, Saveetha School of Engineering, SIMATS, Chennai, 602 105, Tamilnadu, India

^c Radiological Sciences Department, College of Applied Medical Sciences, King Khalid University, Abha 61421, Saudi Arabia

^d Biomaging Unit, Space Research Centre, Michael Atiyah Building, University of Leicester, Leicester, LE1 7RH, UK

^e Research Center for Advanced Materials Science (RCAMS), King Khalid University, Post Code:9004, Zip code: 61413, Abha, Saudi Arabia

^f Electrical Engineering Department, College of Engineering, King Khalid University, Abha 61421, Saudi Arabia

ARTICLE INFO

Keywords:

Milled
Irradiated
Mechano
Electronic
Displays

ABSTRACT

Single crystals of organic type of NLO crystalline material of DBNT - 8, 9-Dimethoxybenzo[b] naphtho [2,3-d] thiophene are proceeded to be grown by slow evaporation procedure and milled to micro scale and irradiated of Co-60 source of 100 Gy, 500 Gy and 5000 Gy for better scope of classification of system of the monoclinic type of DBNT-pure, micro and irradiated ones. The hardness study specifies the reverse indentation size effect (RISE) with work hardening coefficient above two of all DBNT specimen leads to the micro-tribological workings for springs with proper elastic parameters; the transmittance of DBNT of 5 specimens are 321 nm, 323 nm, 341 nm, 351 nm, and 352 nm for macro, micro, 100 Gy, 500 Gy, 5000 Gy. The photonic utility of identity for 3.86 eV and is 3.8629 eV by the transmittance data. The Non Linear Optical - NLO component this of 1.9, 1.94, 1.95, 1.96, 1.99 times that of KDP from which phase matching provision is enabled the influx property for the DBNT specimens is in the order of microns the (110) and (111) indexing represent for display device configuration. The dielectric behaviour of DBNT shows that polarization properly enabled for all categories by electrical performance, the abnormal variation is due to the vacancies created in the molecule by irradiation.

1. Introduction

Over the past decennium, crystal engineering focussing a major role of packages of atom, atomic configuration vital usage in science and techno fields and added privileges is the class of NLO materials and their provoking in the new generation [1–4]. Organic materials are classified as carbon-based materials/composites. They are mainly from organism and major level represented by type of bonding as covalent nature [4–9].

The application is of significance for opto-electronic based or type of material. They exhibit high level of delocalized electrons and large susceptibility. Organic material phase is important role in their growth and mainly employed in laser action, wave guide, light emitting transistor. The π - π^* transition enables the core representation of organic classification of the samples and DBNT is one of the versatile types of specimen [10–15].

* Corresponding author.

E-mail addresses: mcsgoldmedalist@yahoo.in, senthilkannank.sse@saveetha.com (S. K).

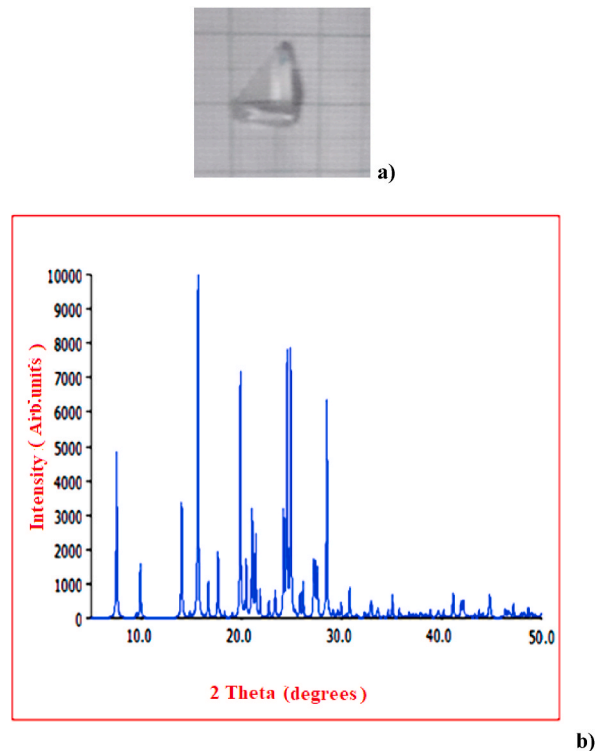


Fig. 1. Photograph and the powder XRD pattern of DBNT crystal.

Table 1

XRD data of DBNT for all samples.

Samples	a, b, c	β	$\alpha = \gamma$
DBNT- Macro	13.0063 Å, 5.9632 Å, 18.3802 Å	104.020°	90°
DBNT - 100 Gy	13.0103 Å, 5.9670 Å, 18.3834 Å	104.034°	90°
DBNT - 500 Gy	13.0115 Å, 5.9688 Å, 18.3852 Å	104.038°	90°
DBNT - 5000 Gy	13.0124 Å, 5.9697 Å, 18.3869 Å	104.043°	90°

The materials possess class of non-centrosymmetric of second order and Z-scan studies and can be projected utility in modulating circuit, opto-electronic gadgets, laser, and frequency converters and so on. Organic NLO of preferred over paired materials for the device converting and also in storage devices.

Our predominant objectivity is the representation of growth of macro, micro and irradiated DBNT specimen and correlate them for better scope of XRD, UV-visible, NLO, phase matching, multiplying circuit, hardness of the versatile scaling of the DBNT correspondingly [10–17]; measured for single XRD by Bruker Kappa Apex II diffractometer; NLO by Q switched Nd-YAG laser, phase matching by NLO SHG parameters and electronic components for multiplier circuits and hardness by Shimadzu HMV 2T and UV-Visible study by PerkinElmer Lambda 35 spectrometer; compared the data of macro, micro and irradiated ones.

2. Synthesis

The material diethyl 2-[(2-(bromomethyl) benzo[b] thiophen-3-yl) methylidene] malonate is properly added with 1,2-dimethoxybenzene with the dried dichloroethane by way of $ZnBr_2$ in the ambience of room temperature under the nitrogen atmosphere for about 5 h. Slowly poured ice-water and effective recrystallization gives the DBNT within 22 days; after successful milled effect of macro, micro-DBNT is obtained; irradiated with the Co-60 as DBNT-100 Gy; DBNT-500 Gy; DBNT-5000 Gy are obtained [1]. The synthesis process is specified in Fig. 1a with proper pictorial proof for growth. 1,2-dimethoxybenzene, dichloroethane, $ZnBr_2$, diethyl 2-[(2-(bromomethyl) benzo[b] thiophen-3-yl) methylidene] malonate each of 99% purity and growth rate of 4.5454%/day and grown in 22 days.

3. Single crystal and powder XRD studies

The single crystal XRD studies are properly analyzed for DBNT all samples is counter verified using the powder XRD data is

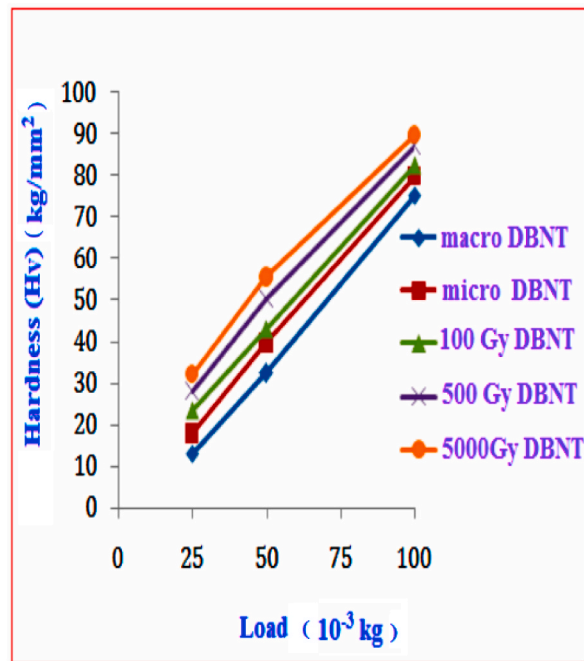


Fig. 2. Hardness profile of versatile DBNT crystals.

Table 2

Hardness profile of versatile DBNT crystals.

Load in 10 ⁻³ kg	Hardness (H _v) in kg/mm ² of DBNT crystals				
	Macro	Micro	100 Gy	500 Gy	5000 Gy
25	13.1	17.9	23.5	28.1	32.2
50	32.4	39.7	43.0	50.2	55.6
100	75.2	79.9	82.6	87.1	89.9

specified in Table .1. The elemental analysis pertaining to the DBNT for the formation, confirmation is represented by the earlier case [1] and is portrayed in Table .1 for comparison and authentication. The DBNT micro-scale is confirmed by the powder XRD pattern with proper values of 2 Theta Vs intensity for the formation of micro-scale and is shown in Fig. 1b. For DBNT- Macro, the parameters are a, b, c as 13.0063 Å, 5.9632 Å, 18.3802 Å and beta as 104.020°; DBNT - 100 Gy, a, b and c as 13.0103 Å, 5.9670 Å, 18.3834 Å and beta as 104.034°; DBNT - 500 Gy, the a, b and c as 13.0115 Å, 5.9688 Å, 18.3852 Å and beta as 104.038°; DBNT - 5000 Gy, the a, b and c as 13.0124 Å, 5.9697 Å, 18.3869 Å with beta as 104.043° corresponding centro-symmetric space group as P2₁/n with monoclinic system.

4. Hardness, tribological data of DBNT crystals

The hardness profile of DBNT crystal in properly analyzed by Vicker's test for five types of DBNT specimen such as macro, micro, 100 Gy, 500 Gy, 5000 Gy as referred with load in 25, 50, 100 g and correspondingly values of H_v for macro, micro and irradiated ones are gradually getting elevated with the values of load 13.1, 32.4, 75.2; 17.9, 39.7, 79.9; 23.5, 43.0, 82.6; 28.1, 50.2, 87.1; 32.2, 55.6, 89.9 kg/mm². This impact the reverse indentation size effect (RISE) for all categories of specimen of DBNT crystals. The corresponding work hardening coefficient 'n' is above the value of 2 and also load is measured in grams and H_v in kg/mm². The load Vs Hardness profile is shown in Fig. 2 and identified in Table .2. The tribological study is in general dealing with wearing effect, tearing effect of the trial which is practically the spherical wire, helically referred springs with DBNT micro-crystalline veneers. The shear value is 0.61 GPa, string's stiffness of 10.2 N/m, shear stress of 3.825 GPa. The parameters correspond to the effective esteems of the entitled sample, and the impactness over the projected use in electronic gadgets/mechano-elastic engineering for existence of the coils or springs for improved strength of trials primarily of micro scales, which is termed as micro-tribology of the DBNT crystals. DBNT of micro and 100 Gy, 500 Gy and 5000 Gy are analyzed and increased value of elastic parameters with increase in irradiation doses is observed and DBNT micro-scale is portrayed for tribological uses with the properly specified values.

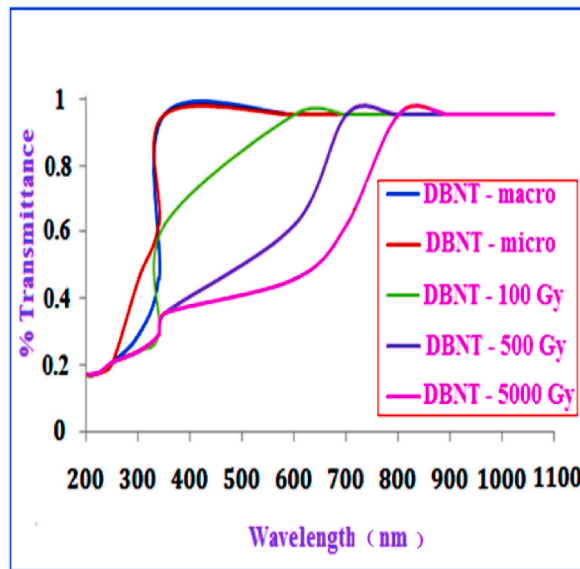


Fig. 3. Transmittance spectrum of DBNT crystals.

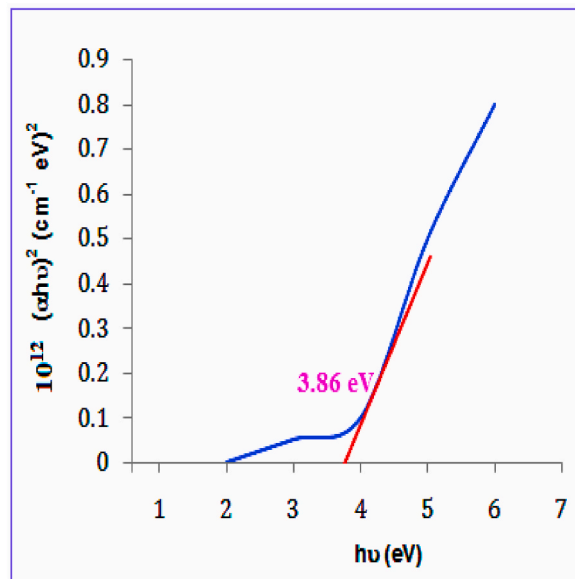


Fig. 4. Photonic utility of DBNT Macro crystal.

5. Optical property and electronic utility of DBNT crystals

UV-visible spectroscopy is a type of spectral outcome especially of the electronic transition level of material for proper measurement of quantity of discrete level of UV or visible nature of light of specified wavelength referred by absorbance or by transmittance. It is a methodology adopted to identify UV-visible region photons and properly referring the intensity after passing through the material as in Fig. 3. The DBNT crystals of scaling such as macro, micro, 100 Gy, 500 Gy, and 5000 Gy, are analyzed for transmittance Vs wavelength in the range of 200 to 1100 nm and the corresponding band gap value in eV; the cut-off values are as 321, 323, 341, 351, 352 nm for macro, micro, 100 Gy, 500 Gy, and 5000 Gy of DBNT. The photonic utility is preceded to measure for all categories of DBNT macro it is in 3.86 eV as in Fig. 4 and by UV-visible spectrum, is in 3.8629 eV as perfectly matched can be further preceded for all the categories Tauc’s plot. The effectiveness is mainly by means of the band gap value. The hardness is clearly specified by the values of data; the UV-visible spectral data pointing out the variations in the spectrum for irradiated samples of three categories and observed the abnormal performance for all, is mainly due to the Co-60 irradiation over DBNT samples and creating vacancy sites

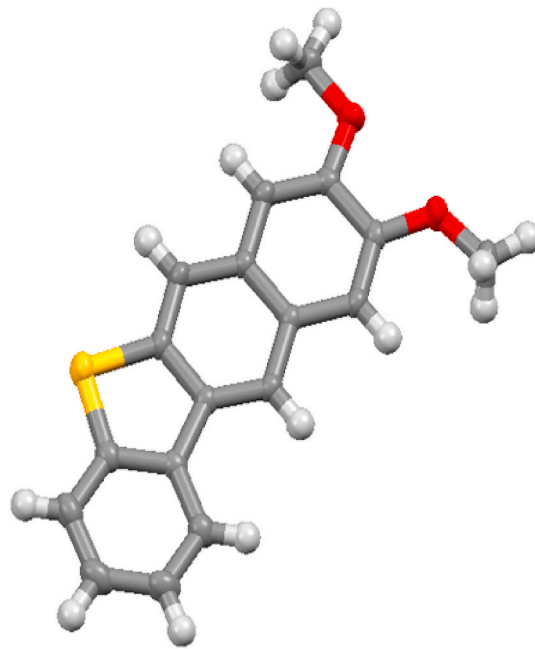


Fig. 5. Molecular structure of DBNT crystal.

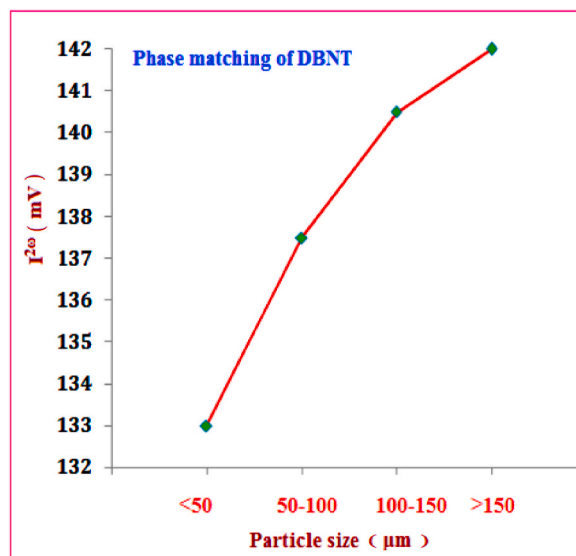


Fig. 6. Phase matching property of DBNT Macro crystal.

may lead to the change over the sample's contour and the peak shifted inference.

The molecular structure pertaining to the DBNT crystal portrayed Fig. 5. The Kurtz powder modulus operandi for the grown DBNT crystal for sustaining the NLO-SHG effectiveness with laser of 1064 nm as the wavelength; DBNT-Macro is properly powdered for all the cases, Macro is 1.9 times [1]; Micro is 1.94 times DBNT-100 Gy, 500 Gy, 5000 Gy are 1.95, 1.96 and 1.99 times of KDP as in Fig. 6. DBNT-Macro third order NLO is 8.9×10^{-6} esu by Z-scan and the phase matching is 133 mV, 136 mV, 137 mV, 138 mV and 140 mV for macro, micro, 100 Gy, 500 Gy and 5000 Gy of DBNT samples. The filter influx of 100 Gy, 500 Gy, 5000 Gy are of 4.8326 μ , 4.9992 μ and 5.2342 μ for opto-electronic filtering specification of the electronic role and the frequency enhance BY-127, BAT-62 are 2.25, 2.31 for micro scale; 2.32, 2.37 for 100 Gy, 2.37, 2.43 for 500 Gy and 2.47, 2.49 for 5000 Gy for proper confirmation of the NLO clause of usage and predominant electronic utility of the irradiated once. The (110) of Miller's indexing for RGB projectile display functioning is specified with 8.9163 Å, the value of Z minimum, Z maximum as 0.0139 and 15.8, maximum saturation as 2.11% and -0.016% as specified in Fig. 7. The (111) of Miller's indexing by Fig. 8 for RGB projectile display functioning is specified with 8.9163 Å, the value of

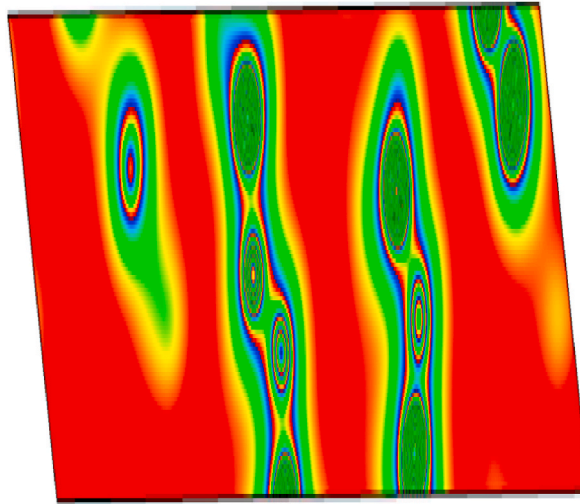


Fig. 7. Display pattern (110) profile of DBNT crystal.

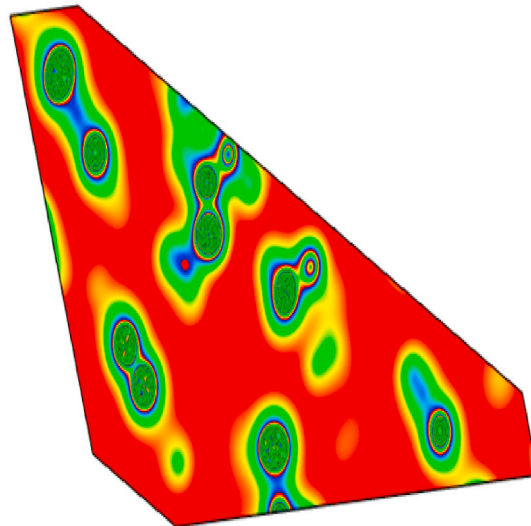


Fig. 8. Display pattern (111) profile of DBNT crystal.

Z minimum, Z maximum as 0.0076 and 29.39, maximum saturation as 2.12% and -0.0164% . For both the modes to specify the devices for display of macro-ones and can be proceeded for other scales too as the values of absolute, recursive colour for proper projection of coloring effect with polygonal ways of triggering by electron gun for projectile television purpose of contrast/brightness, other circuitual adjustment. The centre frequency is 1000 Hz, C1, C2 each of 1000 nano-Farad; $R_1=R_2 = 1000\Omega$, $R_3=R_4 = 40.00 \Omega$ and $R_5=R_6$ as 637Ω , the notch filter calculation gives the Q-factor of 1.989 for normal case for 39.80 as the R_3, R_4 values and Q value is 2.1 times for macro DBNT classification of macro scalings. The Q-factor value depends on the gain function and source of the Op-amp: there is no drift response with the respect to the thermal factors for the notch circuit and frequency response is by R_1 , notching response with the respect to R_6 ; low pass response is by R_4 greater than R_3 ; notching response with $R_3=R_4$; high pass is or R_4 less than R_3 as case of representation. Notch, here refers to allowing particular set of frequency for circuit which contains 3 Op-amps, 6 Resistors, 2 Capacitors developed by Bainter. The effective higher value of Q-factor is mainly by tuned circuitual reference, the DBNT-macro having slightly higher response. This may leads to photo-voltaic and sensing applications.

6. Electrical properties for DBNT

The dielectric behaviour of the DBNT crystal of 100 Gy is studied as the preliminary investigation to proceed for higher doses respectively Figs. 9–15 represents the ϵ_r at frequency depending; $\tan\delta$ as at frequency depending; ϵ_r at temperature depending; $\tan\delta$ at temperature depending; ac conductivity and activation energy correspondingly and Fig. 9 portrays the ϵ_r Vs logf data at variance of

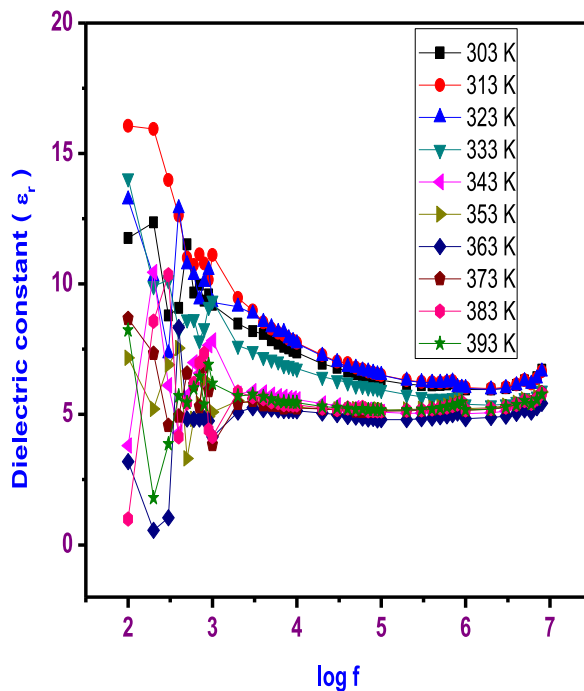


Fig. 9. Dielectric constant Vs logf of DBNT crystal of 100 Gy.

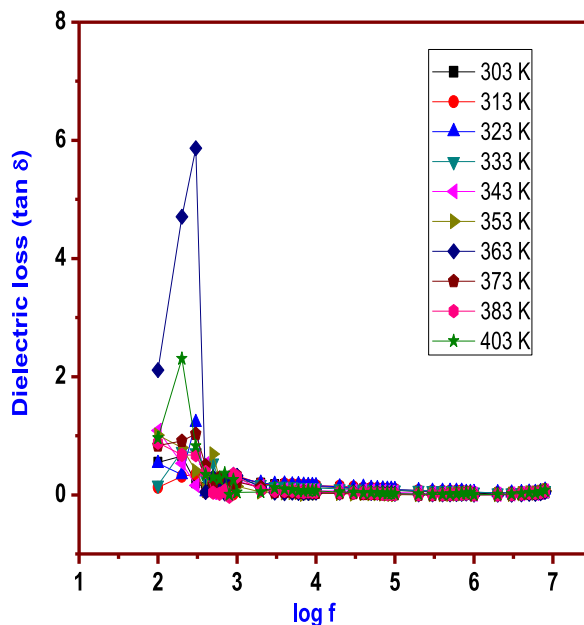


Fig. 10. Dielectric loss Vs logf of DBNT crystal of 100 Gy.

temperature from 303K, 313K, 323K, 333K, 343K, 353K, 363K, 373 K, 383 K and 393K and found that 313K has the ϵ_r max and ϵ_r min value at 383K and for 343K; 303K, the ϵ_r first has lower profile and get enhanced over higher logf data whilst other seven values of temperature is first increased and are gradually in decreasing mode; similarly the dielectric loss profile as in Fig. 10 of $\tan\delta$ Vs logf specifically has the lower value at 333K and higher value at 363K respectively. The variance is by the gamma irradiation by creating vacancy sites depends on dosage and have taken DBNT-100 Gy; DBNT-500 Gy and DBNT-5000 Gy and reported for electrical process of 100 Gy profile and all the polarizations are projected and fitted for the enhanced enrichment of the scaling. Figs. 11 and 12 represent the ϵ_r and $\tan\delta$ for the profile logf Vs Temperature (K) for DBNT-100 Gy sample the value in K are 300–400 in steps of 20K and ϵ_r from

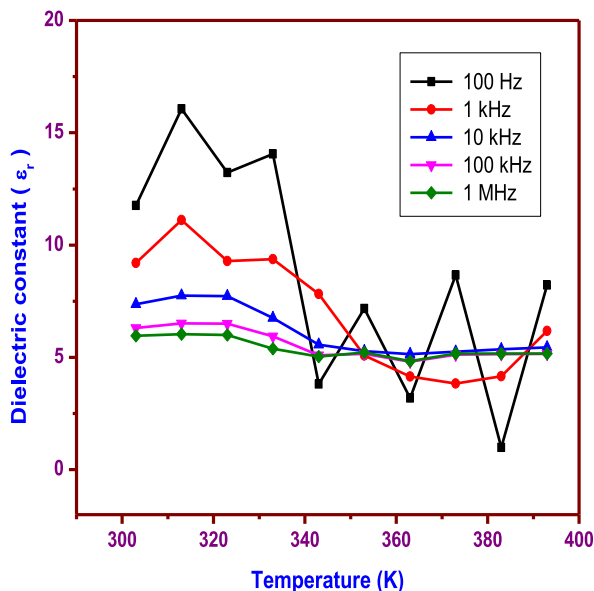


Fig. 11. Dielectric constant Vs Temperature of DBNT crystal of 100 Gy.

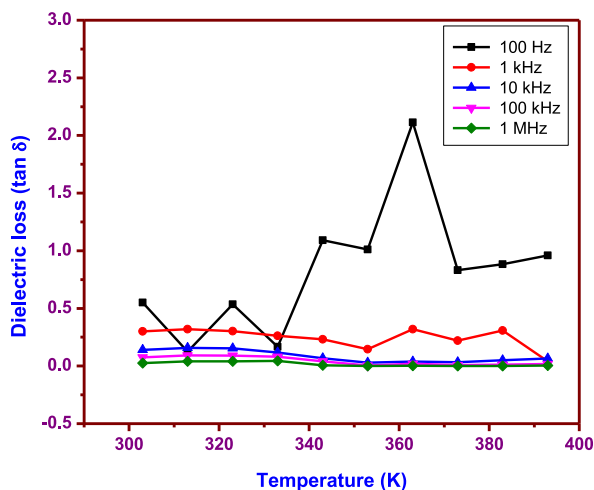


Fig. 12. Dielectric loss Vs Temperature of DBNT crystal of 100 Gy.

0 to 20 in steps of 5; for the frequency in 100 Hz; 1 kHz; 10 kHz; 100 kHz and 1 MHz range and ϵ_r in low at 1 MHz and high at 100Hz; also, the $\tan\delta$ is varied from 0 to 3.0 values and in minimum for 1 MHz and maximum at 100 Hz; the variance as well as the zigzag movement is due to the DBNT-100 Gy radiation by the creation of void sites and projected gap or V or F centers which ultimately results in the abnormal way of outcome in frequency as well as temperature dependence of DBNT. Also, the conductivity as well as the activation energy of DBNT-100 Gy crystal samples specifics the σ_{ac} Vs temperature profile of lower value at 100 Hz and higher value at 1 MHz; as shown in Fig. 13 whilst in σ_{ac} Vs $1000/T$ (K^{-1}) portrays the lower value at 1 KHz (-ve scale) and higher value at 1 MHz (-ve scale) for 100Hz to 1 MHz range as shown in Fig. 14. The activation energy gradually increases with increase in logf values; it is +ve minimum energy measure ups required to get modified as the product of the reactant molecule as shown in Fig. 15. The abnormal variance as well as zigzag motion fits the presence of vacancy sites and void spaces/F and V centers depends on the molecular composite and is due to the gamma ray-100 Gy irradiated over the sample of DBNT and extra-ordinary way of void/notes creates the upper and lower limits variances and projected in this range.

7. Conclusion

The solution growth method is impacted in a great manner to grow the DBNT crystalline specimen and are irradiated with three versatile irradiation in units of Gy and is milled to micro level is of monoclinic crystalline system classification. All DBNT specimens are

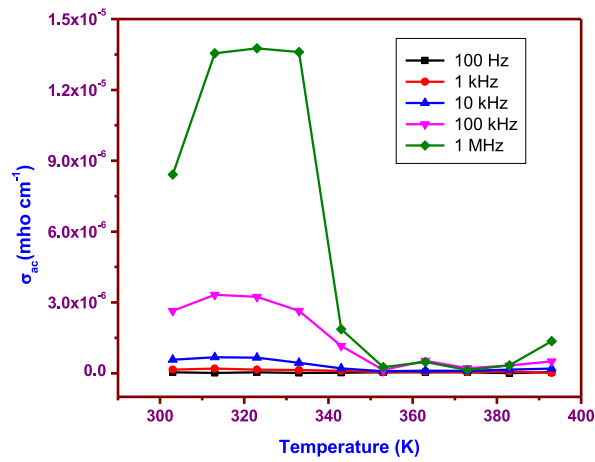


Fig. 13. AC conductivity of DBNT crystal of 100 Gy.

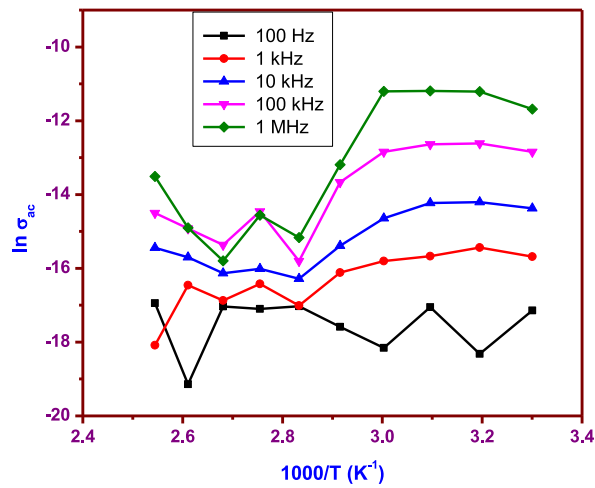


Fig. 14. $\log\sigma_{AC}$ of DBNT crystal of 100 Gy.

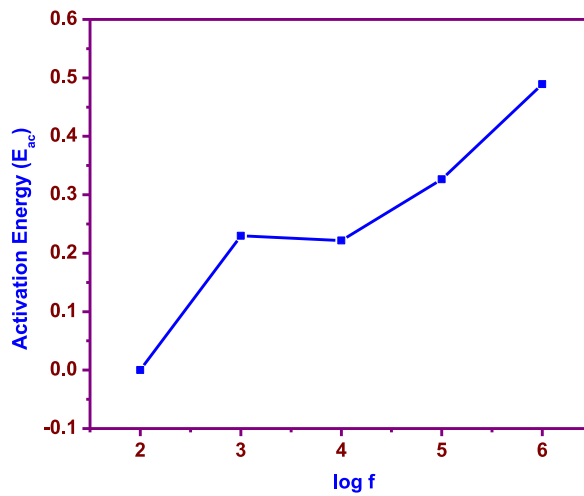


Fig. 15. Activation energy of DBNT crystal of 100 Gy.

related to RISE type of hardness portfolio and the micro-DBNT is relevant for tribological outfit with helical spring elastic parameters. The transmittance wavelength is getting increased from macro, micro, 100 Gy, 500 Gy, 5000 Gy in that order from 321 to 352 nm; the macro photonic classification is confirmed by the 3.86 eV. The NLO component is identified for the DBNT specimen and phase matching provision is also analyzed. The display device confirmation for (110), (111) is represented. The dielectric behaviour is analyzed for all the samples and variation is due to vacancy in the specimen by irradiation. By mechanical work DBNT 5000 Gy is preferred; for transmittance and NLO work, macro and micro is preferred; dielectric nature of 100 Gy only referred and is good impact for electrical outcome than other irradiated samples.

Declarations

Author contribution statement

Meena.M: Conceived and designed the experiments; Performed the experiments.

Senthil Kannan.K: conceived and designed the experiments; performed the experiments; analyzed and interpreted the data; contributed reagents, materials, analysis tools or data; wrote the paper.

Mohammed S. Alqahtani; Mohamed Abbas: analyzed and interpreted the data; Contributed reagents, materials, analysis tools or data.

Data availability statement

No data was used for the research described in the article.

Additional information

No additional information is available for this paper.

Declaration of competing interest

The authors declare that they have no known competing financial interests or personal relationships that could have appeared to influence the work reported in this paper.

Acknowledgement

The authors extend their appreciation to the Research Center for Advanced Materials Science (RCAMS), King Khalid University, Abha, Saudi Arabia for funding this research through the Research Group Program Under the Grant Number:(RCAMS/KKU/025–23).

References

- [1] R. Divya, J. Maalmarugan, R.P. Patel, M. Meena, P. Nikolova, M. Vimalan, et al., *Inorg. Chem. Commun.* 138 (2022), 109249.
- [2] M. Lydia Caroline, R. Sankar, R.M. Indirani, S. Vasudevan, *Mater. Chem. Phys.* 114 (2016) 490, 49.
- [3] P. Jayaprakash, M. Peer Mohamed, M. Lydia Caroline, *J. Mol. Struct.* 1134 (2017) 67–77.
- [4] K. Arunkumar, S. Kalainathan, *Org. Electron.* 77 (2020), 105516, <https://doi.org/10.1016/j.orgel.2019.105516>.
- [5] S.E. AllenMoses, S. Tamilselvan, S.M. Ravi Kumar, G. Vinitha, T. Ashok Hegde, M. Vimalan, S. Varalakshmi, S. Sivaraj, *Mater. Sci. Energy Technol.* 2 (2019) 565–574, <https://doi.org/10.1016/j.mset.2019.05.003>.
- [6] P. Karuppasamy, T. Kamalesh, K. Anitha, M.S. Pandian, P. Ramasamy, S. Verma, *J. Mol. Struct.* 1210 (2020), 128036.
- [7] B. Babu, J. Chandrasekaran, B. Mohanbabu, Y. Matsushita, M. Saravanakumar, *RSC Adv.* 6 (2016) 110884–110897, <https://doi.org/10.1039/C6RA15791B>.
- [8] S. Kalainathan Priyadharshini, *J. Mater. Sci. Mater. Electron.* 28 (2016) 5089–5101, <https://doi.org/10.1007/s10854-016-6222-6>.
- [9] J. Mohana, G. Ahila, M. Divya Bharathi, G. Anbalagan, *J. Cryst. Growth* 450 (2016) 181–189, <https://doi.org/10.1016/j.jcrysgro.2016.06.044>.
- [10] R. Thirumurugan, B. Babu, K. Anitha, J. Chandrasekaran, *J. Mol. Struct.* 1171 (2018) 915–925.
- [11] M.P. Mohamed, P. Jayaprakash, M. Nageshwari, C.R. Kumari, P. Sangeetha, S. Sudha, G. Mani, M.L. Caroline, *J. Mol. Struct.* (2017), <https://doi.org/10.1016/j.molstruc.2017.04.002>.
- [12] S. VEDIYAPPAN, V. Mohankumar, M.S. Pandian, *CrystEngComm* 19 (2017) 5662–5678.
- [13] S. Prince, T. Suthan, C. Gnanasambandham, *J. Electron. Mater.* 51 (4) (2022) 1639–1652.
- [14] K. Suganya, J. Maalmarugan, R. Manikandan, et al., *J. Mater. Sci. Mater. Electron.* 33 (2022), 19320, <https://doi.org/10.1007/s10854-022-08770-0>.
- [15] V. Sathiyaa, K. Suganya, K. SenthilKannan, et al., *J. Mater. Sci. Mater. Electron.* 33 (2022), 19514, <https://doi.org/10.1007/s10854-022-08787-5>.
- [16] X. Vasanth Winston, D. Sankar, K. SenthilKannan, et al., *J. Mater. Sci. Mater. Electron.* (2022), <https://doi.org/10.1007/s10854-022-08873-8>.
- [17] V. Kalaipoonguzhali, S. Surendarnath, M. Vimalan, et al., *J. Mater. Sci. Mater. Electron.* 34 (2023) 107.